16th World Conference on Earthquake Engineering, 16WCEE 2017
Santiago Chile, January 9th to 13th 2017
Paper N° 2274
Registration Code: S-A1464750361

SHAKE-TABLE TESTING AND ANALYTICAL MODELING OF A FULL-SCALE, 4-STORY UNBONDED POST-TENSIONED CONCRETE BUILDING

S. Gavridou[1], J. W. Wallace[2], T. Nagae[3] and T. Matsumori[4]

[1] *Lecturer, Dept. of Civil and Environmental Engineering, University of California, Los Angeles, CA, sgavridou@ucla.edu*
[2] *Professor, Dept. of Civil and Environmental Engineering, University of California, Los Angeles, CA, wallacej@ucla.edu*
[3] *Associate Professor, Disaster Mitigation Research Center, Nagoya University, Japan, nagae@nagoya-u.jp*
[4] *Senior Researcher, National Research Institute for Earth Science and Disaster Prevention, Japan, taizo@bosai.go.jp*

Abstract

This paper presents experimental results from a dynamic test on a full-scale, four-story precast concrete building that utilized unbonded post-tensioned (UPT) walls in one principal direction of response and bonded post-tensioned concrete frames in the orthogonal direction. The building was subjected to simultaneous three-dimensional shaking on the E-Defense shake-table in Japan, using recorded ground motions from the 1995 Kobe earthquake. The excellent performance of the test building in the wall direction of response, exhibiting minimal damage and no residual deformations, confirms that UPT walls are a viable alternative to conventional reinforced concrete (RC) structural walls.

In addition to providing experimental evidence of seismic performance of UPT walls incorporated into a building system, the tests provided valuable insight into issues typically not addressed in component-level experimental studies, such as the role of the floor diaphragm, influence of component interactions, and contributions of three-dimensional responses and torsion. As evidenced by the E-Defense test building, these effects need to be considered to obtain realistic estimates of lateral resistance and displacement demands.

The tests also provided a wealth of data against which design methodologies and analytical models for UPT systems can be benchmarked. An analytical model of the building in the wall direction was developed and experimental results in this direction were used to assess the ability of the model to capture the dynamic responses and interactions of unbonded post-tensioned structural systems. Correlations between analytical and experimental results were satisfactory for a range of global and local responses, and key aspects of the interaction between components such as framing action and beam elongation effects were adequately reflected in the model.

Keywords: precast concrete walls; post-tensioning; shake-table tests; E-Defense; analytical modeling

1. Introduction

In response to the need for improved seismic performance of buildings, there has been a growing body of research on self-centering structural systems that can sustain severe earthquake shaking with minimal damage and no (or limited) residual deformations. Unbonded post-tensioned (UPT) precast concrete walls are part of this family of self-centering systems. Similar technologies have been developed for precast concrete frames [1, 2, 3] and have been extended to other construction materials such as masonry, wood and steel [4, 5, 6].

Research on precast concrete seismic systems initiated in the early 1990s with the PRESSS (Precast Seismic Structural Systems) project that culminated with the pseudo-dynamic testing of a 0.60-scale five-story precast building [7]. The PRESSS building utilized coupled UPT concrete walls in one direction (with coupling devices consisting of U-shaped flexural plates between vertical joints) and precast concrete frames with different types of beam-column connections in the orthogonal direction. Subsequent experimental research related to UPT walls mainly focused on behavior of individual uncoupled walls, including UPT walls without energy dissipators [8, 9], with energy dissipators in the form of mild bonded reinforcement [10, 11, 12], and with alternative dissipative solutions [13]. These experimental studies have demonstrated the ability of unbonded post-tensioned concrete systems to achieve large nonlinear deformations expected in strong earthquake shaking with minimal structural damage and minor residual deformations.

In order to ultimately move UPT systems into wider practice it is necessary that such experimental results be accompanied with design and analysis tools suited for design office application. On the design front, a significant step in accommodating UPT structural systems within the ACI 318 context has been achieved with the ACI ITG-5.2 [14] and ACI 550.3-13 [15] standards which provide design recommendations for specific types of UPT precast concrete walls and frames, respectively. Published analytical studies related to UPT concrete systems range from simplified methods to characterize their monotonic response [16, 17] to lumped plasticity and multi-spring models [18], fiber element models [19, 20] and more detailed continuum finite element models [9]. Given the limited experimental data on dynamic responses and interactions of full scale, three-dimensional UPT structural systems, the aforementioned design approaches and analytical models have been primarily validated against static cyclic tests of individual components.

The work presented here adds to the growing body of research aimed at experimental validation of UPT structural systems and provides unprecedented experimental evidence of seismic performance of UPT walls incorporated into an entire building system. The experiment described herein was conducted in 2010 at the E-Defense shake table facility in Japan and included dynamic testing of a full-scale, four-story precast concrete building. The test building utilized UPT walls coupled to corner columns by UPT beams in one principal direction of building response, and bonded post-tensioned concrete frames in the orthogonal direction. The paper provides an overview of the test program and presents experimental results in the wall direction of response. The development and experimental verification of a nonlinear analytical model in the wall direction of the test building is also discussed. In addition to validating the proposed computational model, the analyses allow system interactions such as framing action resulting from coupling of the UPT walls to the corner columns through the UPT beams, and interactions of the UPT beams with the floor system to be quantified. Together with the experimental results, the analyses provide valuable insight into the dynamic responses and interactions of a full-scale, three-dimensional UPT wall building.

2. Test Program

In December 2010, two full-scale, four-story, concrete buildings were tested under multi-directional shaking on the E-Defense shake-table (Fig. 1a) in Miki, Japan. The two buildings were almost identical in geometry and configuration, and were tested simultaneously. One of the test structures, incorporated conventional reinforced concrete systems (RC structural walls in one direction and RC moment frames in the orthogonal direction) whereas the other structure, referred to as "the PT building" hereafter, was constructed form individual precast concrete members jointed together with post-tensioning steel. Fig.1(b) shows the plan layout of a typical floor of the PT building. Plan dimensions were 14.4 m in the longitudinal (x) direction and 7.2 m in the transverse direction (y). Story heights were 3.0 m at all levels, resulting in an overall height of 12.0 m.

Similar to the RC building, the PT building also used different lateral force resisting systems in the two principal directions. In one direction, two UPT walls, located at opposite sides of the building, acted as the main lateral force-resisting system. Each UPT wall consisted of four precast concrete panels that were vertically stacked and post-tensioned to the foundation with high-strength post-tensioning steel, unbonded over the entire wall height. At the base wall panel, additional mild reinforcing bars (ED bars) were placed across the wall-foundation interface to provide energy dissipation. These bars were deliberately debonded over a distance within the lower wall panel and were anchored within the foundation using grouted couplers. Fig.1(c) shows the cross-section of the UPT wall panel at the base. Non-shrink grout was used at joints between individual precast panels and at the interface between the base panel and the foundation. Steel fibers were included at the wall-foundation interface grout and the concrete mix of the first and second story panels of the north wall. Precast UPT beams on either side of each wall coupled the wall to corner columns at each floor level. The individual single-bay precast UPT beams on either side of the wall were connected by horizontal (unbonded) post-tensioning steel that ran through ducts in the beams and through the wall and columns. An interior one-bay frame (Frame B in Fig.1b) also contributed to lateral resistance in the same direction (wall direction). In the orthogonal direction, lateral resistance was provided by two perimeter two-bay moment frames constructed with precast beam and column elements jointed together with bonded post-tensioning steel. The floor system consisted of precast pre-tensioned double tees spanning parallel to the walls and topped with a cast in-place concrete slab.

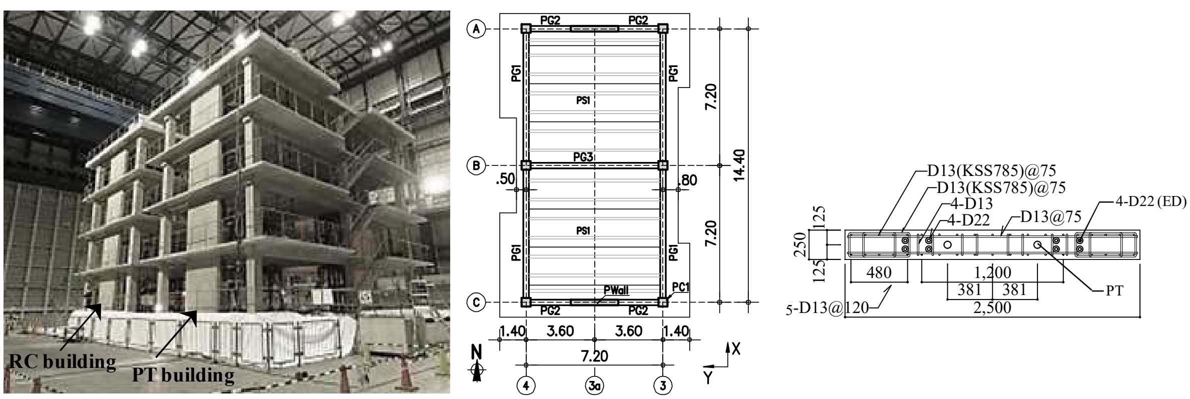

(a) (b) (c)

Fig.1 - (a) RC and PT buildings on shake table; (b) typical framing plan of PT building (dimensions in m); and (c) UPT wall cross section at base (dimensions in mm).

The two buildings were subjected to four acceleration records corresponding to increasing intensities of the JMA-Kobe (10%, 25%, 50% and 100%) record, followed by two acceleration records corresponding to increasing intensities of the JR-Takatori record (40% and 60%). Fig.2 shows the 5%-damped acceleration response spectra derived from the y-direction acceleration histories for the JMA-Kobe and JR-Takatori records as observed on the shake table. For reference, the design and MCE_R spectra (ASCE 7-10) for a site in downtown Los Angeles (S_s=2.39, S_1=0.84, site class D) are also included in Fig.2. Both structures were heavily instrumented and a total of 609 channels of data were collected during the tests including accelerometers, displacement transducers, and strain gauges. The tests provided a wealth of data to assess behavior of RC and UPT components under multi-directional dynamic loading and to investigate system interactions. This study focuses solely on the response of the PT building and specifically on the behavior in the direction that utilized UPT walls as the lateral-force-resisting system (y direction). Additional information on the design, construction and instrumentation of the test buildings can be found in [21] while the digital data from the experimental program are available on NEEShub website (NEEShub project 2011-1005).

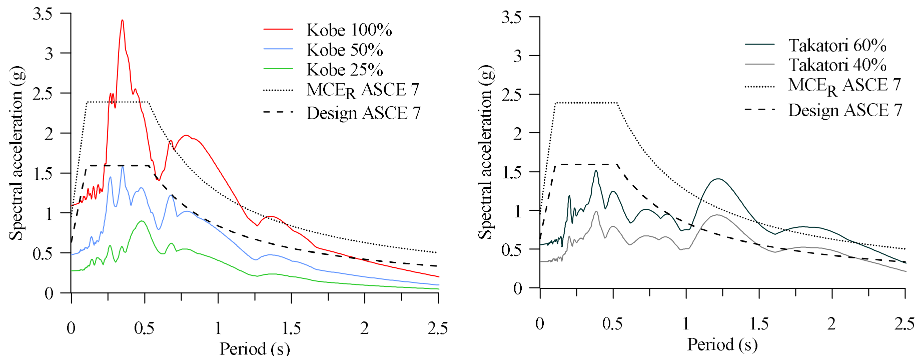

Fig.2 - 5%-damped acceleration response spectra of input motions.

3. Experimental Results in the Wall Direction of Response of the PT Building

Performance of the PT test building in the wall direction was very satisfactory. Consistent with the expected behavior of UPT systems, inelastic demand was generally concentrated at the jointed connections between the precast members and, upon completion of the tests, no significant residual deformations were observed, confirming the inherent re-centering properties of UPT systems.

Fig.3(a) shows the observed damage in the y-direction of the building after the 100%-Kobe record. No visible damage was observed at the end of the lower intensity tests. Apart from the intended single crack at the base, the north UPT wall (axis A) remained essentially intact under the 100%-Kobe record and only minor cosmetic spalling occurred at the east end of the base panel (Fig. 3b). The fiber reinforced interface grout at the base of the north wall also remained intact as it moved upward together with the lowermost precast panel. In the south UPT wall (axis C), which did not contain fiber reinforcement, the 30-mm thick grout pad along the base joint partly crushed and spalled during the 100%-Kobe record. This resulted in the lowermost precast panel to separate from the grout and gap opening to develop at the base of the wall panel (as opposed to the base of the grout pad). As shown in Fig. 3(c), spalling of concrete cover occurred at the corners of the south UPT wall and extended above the foundation over a height approximately equal to the thickness of the wall. Although lack of fiber reinforcement adversely affected the behavior of the south wall and led to faster degradation, damage in the south wall was still repairable and localized at the base. No cracking developed at the upper portion of the lowermost panel or in the upper story precast panels that remained essentially elastic. Moreover, despite the partial crushing of the interface grout, no prestress losses occurred and no sliding was observed at the base of the south wall. This level of performance is still superior to expected performance of conventional RC walls under same intensity seismic actions [22].

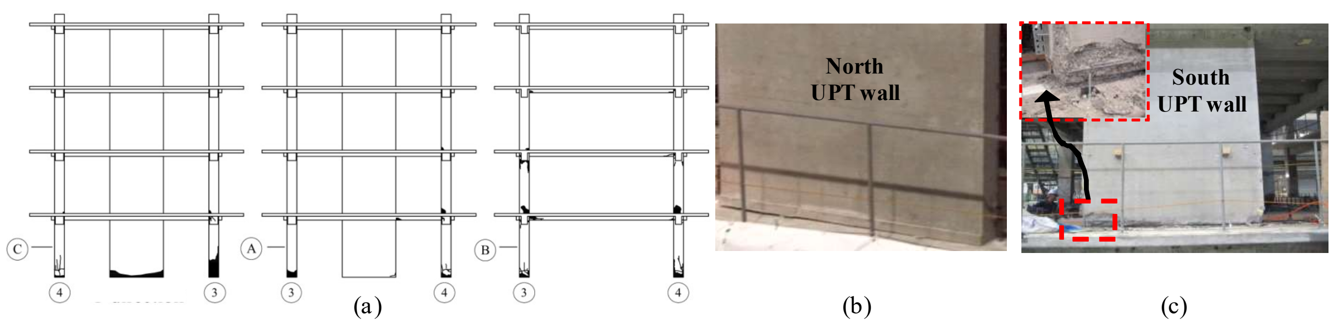

Fig.3 - (a) Observed damage in y-direction of PT building after the 100%-Kobe record; (b) condition of north UPT wall at end of tests; (c) condition of south UPT wall at end of tests.

The UPT beams in the y-direction of the PT building generally performed as intended, with nonlinear deformation mainly concentrated at the beam-column and beam-wall connections and limited spalling of concrete cover at the bottom faces of beams adjacent to the columns and wall. Interaction and displacement incompatibilities between the slab and the UPT walls and beams in the test building also led to some slab damage during the tests. Other damage observed after the 100%-Kobe record included concrete crushing at bases of first story columns and axis-B second-story columns. This damage was mainly associated with the frame (x) direction of response that subjected the columns to peak interstory drifts more than two times higher than the y-direction peak drifts.

The following subsections present experimental results for a range of responses in the wall direction of the PT building including global force-displacement relations and local behaviors such as wall base rotations and wall uplift. Additional information can be found in [23].

3.1 Global hysteretic response

The global hysteretic response in the wall (y) direction of the PT building is illustrated in Fig.4(a), in terms of global overturning moment versus roof drift at the center of plan. Response under low intensity shaking, represented by the 25%-Kobe record, was essentially linear elastic. Slightly nonlinear behavior was obtained under the 50%-Kobe record and was mainly associated with softening due to gap opening along the horizontal joints at the bases of the UPT walls. The narrow hysteretic loops and limited energy dissipation are consistent with the characteristic nonlinear elastic response expected of unbonded post-tensioned systems before significant yielding of the energy-dissipators occurs. Also consistent with the expected behavior of UPT systems under moderate to high intensity shaking, no visible damage was observed at the end of the 50%-Kobe test and complete self-centering response was achieved. The majority of inelastic response and energy dissipation occurred during the 100%-Kobe record. Modest strength degradation was observed after the first excursion exceeding 1.0% roof drift in each direction. After the first two large excursions in each direction, considerable degradation of the initial stiffness also occurred. Hysteretic loops obtained during the final tests under the Takatori records displayed the same (degraded) stiffness observed at the end of the 100%-Kobe record, without significant additional degradation in strength. Residual displacement was negligible at the end of the tests.

3.2 Response envelopes

Fig.4(b) plots the interstory drift ratio envelopes at the center of plan. Distribution of drift was almost uniform along the height of the building for all records and peak interstory drift ratio during the tests was 1.66% (at center of plan). Fig.4(c) shows the building moment in the wall direction of response for each record along with design values for overturning moments (M_u). These design values correspond to base shears of 0.2W and 0.3W for the DBE and MCE level, respectively, and a vertical distribution of seismic forces according to 12.8.3 of ASCE 7-10. Fig.4(c) also plots the moment capacities (M_n and M_{prob}) of the two UPT walls according to ACI ITG-5.2. Calculated moment capacities M_n and M_{prob} exceed the design demands M_u at DBE and MCE, respectively; however, the experimental moments are significantly higher than the calculated wall moment capacities. The peak overturning moment of the building during the tests was almost two times the probable moment strength at the bases of the UPT walls. This difference can be largely attributed to interaction of the walls with the UPT beams that framed into them and coupled the walls to the corner columns at each floor level. Prior testing has shown that even gravity framing and coupling through slabs can have a similar effect on lateral resistance and shear demands of both UPT and RC wall systems [24, 25]. In addition to the wall capacities and framing action (axial force couple at the bases of Frame A and C columns), other sources adding to the lateral resistance of the test building include moment resistance at the bases of the columns and contribution of the intermediate one-bay moment frame (Frame B). Analytical studies presented in Sections 4.3 and 4.4 quantify, by means of a nonlinear model of the building, the relative contributions of various sources to moment resistance and assess the impact of framing action on wall shear demands.

3.3 Displacement profiles

Fig.5 shows the displacement profiles along the height of the building at peak roof drift for each record. Profiles are almost linear, verifying that displacement response was largely dominated by rigid body rotation (rocking). Three lines are plotted for each record: the displacement at the center of plan, and the story displacements at the north and south ends of the building. For each record, all displacement values shown are simultaneous and correspond to the instant at which the peak roof displacement occurred at the center of plan. Profiles of Fig.5 indicate a notable torsional response of the building; displacements at the south end were consistently larger than north end displacements and differences increased with increasing level of seismic intensity. At low intensities, variations of material properties and unintended mass eccentricity related to locations of non-structural elements in the building may have contributed to the torsional response of the building. For the 100%-Kobe and Takatori records, the earlier degradation of concrete and grout in the south wall and subsequent different behaviors at the base joints of the two UPT walls likely increased the torsional component of displacement and resulted in the south wall sustaining significantly larger displacement demands than the north wall.

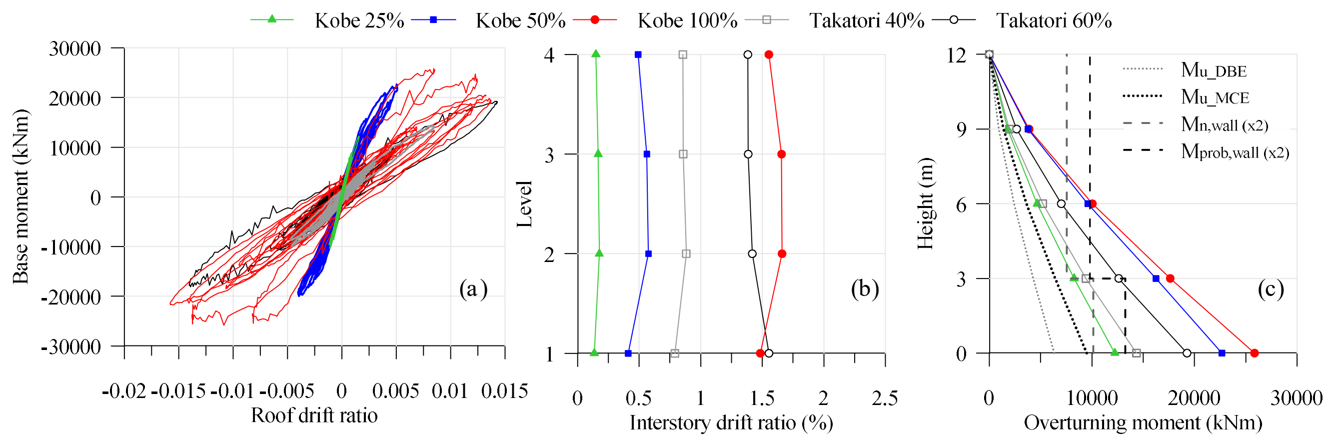

Fig.4 - (a) Global hysteretic response in y-direction of PT building; (b) interstory drift ratio envelopes; (c) overturning moment response envelopes.

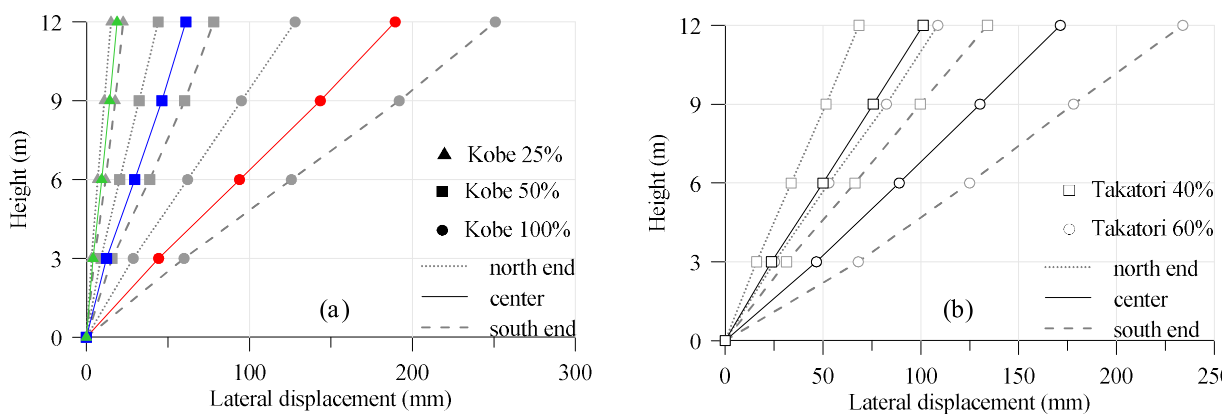

Fig.5 - Displacement profiles at peak roof displacement for (a) Kobe and (b) Takatori records.

3.4 UPT wall responses

Fig.6(a) compares the (in-plane) base rotation histories of the two walls under the 100%-Kobe record. Differences between south and north wall rotations are more pronounced after the first two large excursions in each direction when crushing of the grout pad and spalling of concrete cover occurred at the base of the south UPT wall. The peak rotation of the south wall occurred at t =20.1 s and was equal to 1.94%. At that instant, the rotation of the north wall was only 0.89%. Also shown in Fig 6(a) is the out-of-plane rotation history at the base of the south wall. As evidenced by the plot, out-of-plane rotations significantly exceeded in-plane rotations. Note that wall out-of-plane rotations are consistent with measured story lateral displacements in the frame (x) direction of the test building where peak drift ratios of 3.90% were measured for the first story under the 100%-Kobe. Despite their large magnitude, the out-of-plane drifts in the moment frame direction did seem to adversely affect the in-plane behavior of the UPT walls. Upon completion of the tests, no visible flexural cracks were observed in the walls, and test observations and videos from cameras providing close-up views of the UPT wall bases confirmed that drifts in the moment frame direction were largely accommodated by out-of-plane rocking of the walls against the foundation. Fig.6(b) compares the base rotation versus east end uplift of the two walls under the 100%-Kobe record. Despite the different amplitudes, behavior of the two walls in terms of rotation-uplift relations was very similar. Fig.6(c) shows response histories of concrete strains at the west ends of the south and north UPT walls under the 100%-Kobe record. These represent average strains over the 250-mm gauge length of vertical sensors (D2) at the west end of the walls. Peak concrete strains at the west end of the south and north UPT walls were 0.025 and 0.008, respectively.

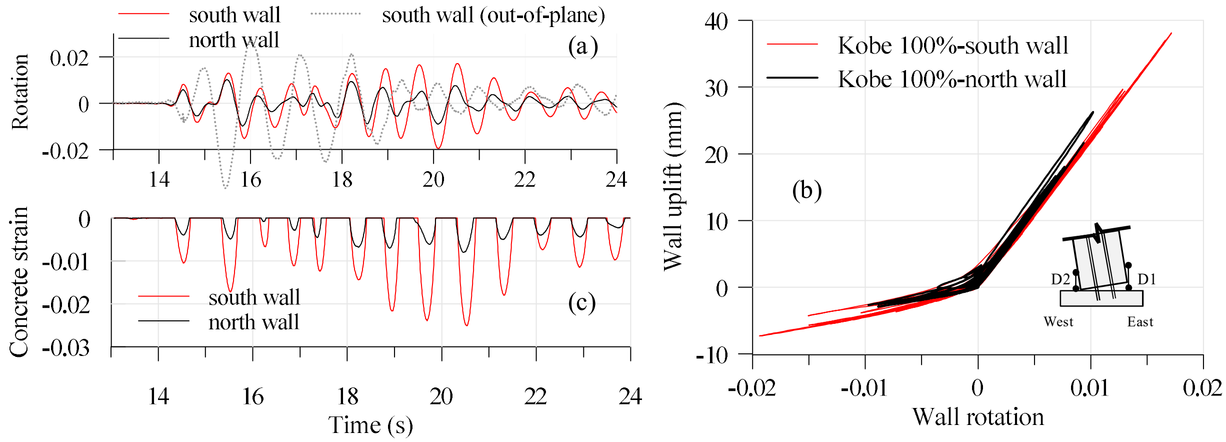

Fig.6 - Wall responses under 100%-Kobe record: (a) wall base rotation histories; (b) wall uplift at east end versus rotation; (c) wall concrete strain histories at west end.

4. Analytical Model in the Wall Direction of Response of the PT Building

As experimental investigations on dynamic behavior and interactions of UPT systems are limited to-date, the 2010 E-Defense tests provided unique data against which analytical models for UPT systems can be benchmarked. This section describes the development of an analytical model of the E-Defense test building and presents comparisons between analytical and experimental results. Using results from the analytical model the relative contributions of various sources to moment resistance are quantified and the impact of framing action on wall shear demands are assessed. More detailed information on the analytical studies is available in [23].

4.1 Development of analytical model

Although the building was subjected to simultaneous multidirectional shaking (x, y, z), this paper focuses solely on the response in the direction that utilized UPT systems (y-direction). To this end, an analytical model that includes the frames along axes A, B and C (Fig. 7a) was developed in Perform3D [26] and subjected to the y-direction accelerations observed on the shake-table during the test.

The UPT walls were modeled using a combination of inelastic shear wall elements and truss elements. Shear wall elements in Perform3D are 4-node macro-elements organized in two layers acting in parallel: an axial-bending layer and a shear layer. The axial-bending layer is described by fiber sections consisting of concrete and steel fibers described by uniaxial stress-strain relationships. The shear layer is defined by a shear material, described by a shear stress-shear strain relationship, and is based on the assumption of constant shear stress in each element.

Gap opening at the base of the UPT walls was modeled using shear wall elements with concrete-only fibers (no-tensile strength) over a short distance, H_{cr}, from the base. In this way, gap opening under lateral load was simulated as elongation of the wall concrete fibers that go into tension (positive strain under zero stress). The mild bonded reinforcement of the precast wall panel was not included in the base fiber sections as it did not cross the wall-foundation interface. The effect of transverse reinforcement was accounted for by using concrete fibers with different stress-strain relationships to model the well-confined ends of the base panel compared to the unconfined concrete within the middle portion (web) of the panel. A value of H_{cr} equal to the thickness (t_w) of the walls was used. H_{cr} represents the height above the base over which nonlinear behavior of the concrete in compression is expected to extend. Selection of H_{cr} was based on observed damage at the base of the south UPT wall, where concrete spalling extended vertically for a distance approximately equal to t_w. The selected value for H_{cr} also coincides with the gauge length of the vertical sensors provided at the wall ends, thus facilitating comparisons of analytical and experimental local responses. Above the height H_{cr}, any reinforcement that was bonded and adequately developed was included in the wall fiber sections. Shear behavior was modeled using an elastic uncracked shear modulus ($G_c=0.4E_c$, where E_c is the modulus of elasticity of concrete) as the majority of lateral displacements in UPT walls is attributed to rocking at the critical interface and contribution of shear deformations is expected to be small.

The unbonded PT steel and unbonded length of the energy dissipating (ED) bars were implemented as vertical inelastic truss elements, placed outside of the wall fiber section as strain compatibility is not enforced between concrete and steel over the unbonded lengths. Nonlinear force-deformation relationships that approximate the actual stress-strain relations from material characterization tests were assigned to the truss elements and the pre-stressing force was simulated as an element load (initial strain) in the PT bars. The ED truss elements had common nodes with the wall elements at the top and were pinned below the wall base at a distance that accounts for an additional debonded length due to strain penetration. The PT truss elements were pinned at the base, accounting for the additional unbonded length inside the foundation, and connected through rigid links to the adjacent wall nodes at the top of the wall.

The prestressed columns were modeled using inelastic fiber column sections with the area of bonded PT steel included in the fiber section. The UPT beams were modeled using a combination of inelastic beam fiber sections and horizontal inelastic truss elements. Gap opening at critical interfaces was modeled using beam fiber segments with concrete-only fibers (no-tensile strength) over a critical length, L_{cr}, at each beam end. Outside the length L_{cr}, any beam reinforcement that was bonded and adequately developed was included in the beam fiber section. A value of $L_{cr}=0.4h$, where h is the beam depth, was used based on (average) observed horizontal extent of damage to the UPT beams from the wall or column interface. The unbonded PT steel of the UPT beams was modeled using horizontal inelastic truss elements with initial strain to simulate the prestress. Vertical rigid links at the locations of the PT steel anchorages at the external faces of columns connected the end nodes of the PT truss elements to the adjacent beam element nodes.

With the intent of capturing the effect of the in-plane action of the floor system in partially restraining gap opening at beam ends, the slab was explicitly modeled. Elastic shell elements with an effective membrane thickness equal to 25% of the gross section thickness were used as the restraint provided by the slab is likely to reduce once cracking occurs. In this implementation, the restraint of beam axial growth is provided by the in-plane action of the slab elements as follows: gap openings at the ends of the UPT beams, implemented in the model as extension of the beam concrete fibers at the critical interfaces, cause the overall length of the beams at the vertical location of the slab elements (mid-depth of cast-in-place slab) to increase, and consequently tensile forces to develop in the slab. In [23] it is shown that, depending on the in-plane stiffness of the slab, these forces can have a significant impact on beam moment capacities. Sensitivity of both global and local responses to the in-plane stiffness of the slab is also examined in [23] and briefly discussed in Section 4.4.

Seismic masses were distributed to slab nodes at each floor level. Gravity loads were applied as point loads on wall and column nodes and prestress forces as initial strains on truss elements implementing the PT steel. P-Delta effects were included. Rayleigh damping was used with damping ratios of 2.5% at $0.2T_1$ and $1.5T_1$, where T_1=0.27s is the calculated (elastic) fundamental period in the wall direction of response. Analyses were run in sequence: after application of gravity and prestress forces, the sequence of Kobe records (25%, 50%, 100%) was run.

4.2 Comparisons of analytical and experimental results

Figs. 7(b)-7(d) compare analytical and experimental responses for the 100%-Kobe record under which the majority of inelastic response occurred. Fig. 7(b) shows the analytical and experimental response histories of roof drift ratio in the wall direction of response of the test building while Fig. 7(c) compares base moment versus roof drift relations determined from the analysis with those extracted from the experimental data. Experimental roof drift ratios correspond to the geometric center of the building plan. As discussed in Section 3.3 significant torsional response was observed during the experiment and was mainly attributed to different behaviors at base joints of the two UPT walls due to lack of fiber reinforcement in the wall-foundation interface grout and concrete mix of the south wall. As a result, the south wall in the experiment sustained earlier degradation and larger displacement demands than the north wall. This behavior is not reflected in the analytical model where the grout was not explicitly modeled and identical behaviors were assumed for the south and north UPT walls. Comparisons between results from this symmetric model and experimentally measured drifts at the center of plan are conditioned on the assumption that torsion did not affect the center of mass displacement. Fig.7 (c) shows that peak overturning moment and peak displacements at the center of plan are well predicted. However, the analytical model displays earlier softening than what was observed in the test; this can be attributed to the effective stiffness value assumed for the slab (also refer to Section 4.4). Furthermore, the model tends to recover the initial stiffness at small drifts and thus exhibits a more pronounced flag-shaped response compared to the test results; a possible explanation is related to bidirectional effects not captured in the model. Due to torsional response, measured response histories of local wall and beam responses are not directly comparable to analytical response histories. However, it was possible to use experimental data to validate the local behavior of components in the model, such as the base uplift versus wall rotation relation for the walls (Fig. 7d). Despite differences in magnitude, associated with torsion, Fig. 7(d) shows that the overall behavior of the UPT walls was adequately captured in the analytical model.

4.3 Decomposition of base moment resistance

Using analytical results for the 100% Kobe record, Fig. 8(a) plots the distribution of base moment between the exterior two-bay frame consisting of the UPT wall, UPT beams and corner columns (Frame A), and the interior one-bay frame (Frame B). Due to symmetry in the analytical model, response of Frame C is identical to Frame A. The contributions from the three frames add up to the total base moment resistance of the building, previously plotted in Fig. 7(c). At the instant of peak strength, the interior frame accounts for 10% of the total base moment resistance with the remaining 90% provided by the two exterior frames, which also accounted for the majority of hysteretic energy dissipation in the building. Further decomposition of Frame A resistance into its components (Fig. 8b), namely the wall moment, column moments, and moment from the force couple produced by the axial loads at the column bases, shows a significant contribution of the force couple. The moment resistance from the force couple, referred to as framing action herein, is directly related to the end moments and corresponding shear forces of the UPT beams as the magnitude of the (seismic) axial load at the base of each column equals the sum over all floors of the shear forces of the framing UPT beams. Combining results from Figs. 8(a) and (b), the building's total moment resistance at the instant of peak strength during the 100%-Kobe record, can be decomposed into the following contributions: 22.5% from the moment capacity at the base of each UPT wall, 17.5% from framing action at each exterior frame, 5.0% from the column moments at each exterior frame and, finally, 10% contribution from the interior one-bay frame.

4.4 Framing action and slab effects

Given the large contribution of framing action to the overall resistance in the wall direction of the PT building, Fig.8(c) examines, by means of pushover analyses, sensitivity of analytical results to the assumed effective stiffness of the slab. The"25-mm slab" model in Fig.8(c) coincides with the analytical model described in Section 4.1 (effective slab thickness equal to 25% of the gross thickness of the 100-mm cast-in-place slab). It is noted that framing action in the context considered herein, is solely dependent on beam moments and corresponding shears, which in turn, are largely affected by the in-plane stiffness of the slab as described in Section 4.1. Fig. 8(c) shows that at small drifts (<0.2%), slab effects had no impact on global responses as beam rotations and beam axial growth were not sufficiently large to activate the restraint by the slab. For drift ratios between 0.2% and 1.2%, increasing the effective slab thickness increased beam moment capacities by up to 2.5 times and overall moment resistance of the building by up to 35% (at 1.0% drift ratio). At larger drifts, increases in effective slab thickness did not result in further increase of moment resistance, as the induced axial forces in the beams cause crushing of the concrete in compression at the bottom of the beams, which increases the neutral axis depth and limits beam moment capacities. Finally, it is also of interest to examine the effect of in-plane stiffness of the slab on wall shear demands. Using analytical results from models with different degree of framing action, similar to those presented in Fig. 8(c), it was found that wall base shear increased with increasing degree of framing action and at 1.5% roof drift ratio, the wall base shear predicted by a model using an effective slab thickness of 25 mm is approximately 30% higher than the base shear of the cantilever wall at the same drift. These results show that, although typically ignored in design and analysis of buildings, beam axial growth and slab effects can have a significant impact on responses.

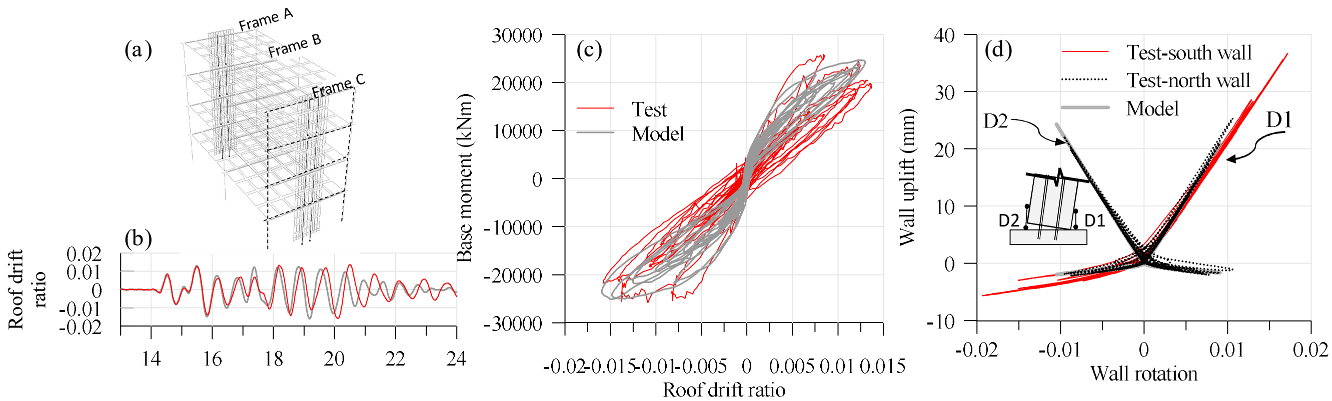

Fig.7 - (a) 3D view of analytical model in Perform3D; Comparisons of analytical and experimental results under 100%-Kobe record: (b) roof drift histories; (c) global hysteretic responses; (d) wall uplift vesrsus rotation.

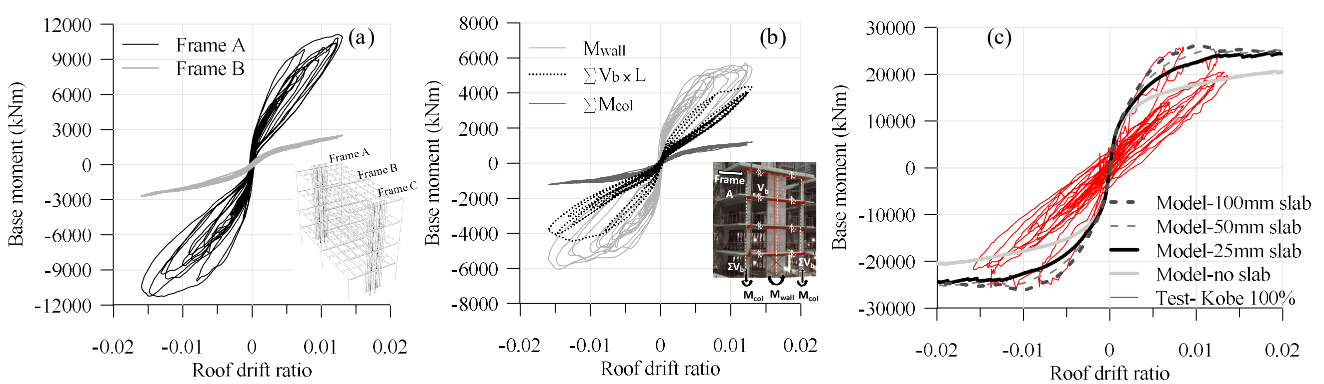

Fig.8 - Decomposition of 100%-Kobe analytical overturning moment: (a) between Frames A, B, C; (b) between Frame A contributions (wall moment M_{wall}, column moments ΣM_{col} and framing action $\Sigma V_b xL$). (c) Effect of slab stiffness on analytical global response.

5. Conclusions

The 2010 E-Defense shake table tests on a full-scale, four-story precast post-tensioned building that utilized UPT walls, added a wealth of data to the limited database on dynamic responses and interactions of UPT systems. The tests provided unique data to assess behavior of UPT walls under multi-directional dynamic loading and investigate system interactions (e.g., wall with UPT beams and slab).

This paper presented experimental results for a range of responses in the wall direction of the test building, with an emphasis on responses of the two UPT walls. Damage to the UPT walls was limited to grout crushing and concrete spalling at the base of the south wall. Apart from this localized and repairable damage, no cracking developed at the upper portion of the wall. Overall response of the building in the wall direction was dominated by gap opening at the bases of the UPT walls (rocking). The peak roof drift ratio was 1.58% at the center of plan while residual drift at the end of the tests was minor. Calculated peak roof drifts for the south

(2.09%) and north wall (1.07%) differed from the center of plan drift due to torsional response. Torsional response was largely associated with differences in performance of the base joints of the two UPT walls due to lack of fiber reinforcement in the south wall. These differences verify that response of UPT walls is mainly governed by the behavior of the wall-foundation joint. By ensuring that inelastic action due to high compressive forces at the critical joint can develop in a ductile manner, without significant degradation of concrete or grout, an essentially damage-free structural system can be obtained.

The development and experimental validation of an analytical model of the E-Defense test building was also presented. The model used a combination of inelastic fiber sections (for walls, beams and columns), inelastic truss elements (for unbonded PT and ED steel) and elastic slab elements. Overall good simulations of observed global and local responses were obtained, with satisfactory correlations between predicted and measured roof displacements, overturning moment, and base uplift versus wall rotation relations for the walls. Decomposition of base moment resistance of the building into its components showed that coupling of the walls to the corner columns, through the UPT beams and slab, contributed significantly to lateral resistance of the building in the wall direction (approximately 35%). Contribution of framing action was accentuated by interactions of UPT beams with the floor system. By restraining beam axial growth, the slab induced axial compressive forces in the beams that increased beam flexural capacities and framing action. It was shown that although typically ignored in design and analysis of buildings, framing action and axial growth effects can have a significant impact on responses and need to be evaluated to obtain realistic estimates of force and displacement demands. Together with the experimental evidence of seismic performance of UPT systems documented in this paper, the analytical studies provide valuable insight into system interaction issues that are generally not addressed in component-level analytical and experimental studies, but are likely to occur in both UPT and conventional RC buildings.

6. Acknowledgements

The authors acknowledge the generous support of the Ministry of Education, Culture, Sports, Science & Technology (MEXT) as well as the National Research Institute for Earth Science and Disaster Prevention of Japan in carrying out the test presented in this paper. Participation of the American co-authors in the project was supported in part by Pacific Earthquake Engineering Center as well as the Network for Earthquake Engineering Simulation of the National Science Foundation under award CMMI-1000268, whereas funding for NEES@UCLA instrumentation was provided under award CMMI-1110860. The authors would like to acknowledge Dr. S. Sritharan of Iowa State University and Professor T. Kabeyasawa at the Earthquake Research Institute at the University of Tokyo for providing additional instrumentation for the test buildings, as well as Dr. Richard Sause and his former PhD Student, Wesley Keller, at Lehigh University for conducting the pre-test analytical studies on the PT building. Opinions, findings, conclusions, and recommendations in this paper are those of the authors and do not necessarily represent those of the sponsors or other individuals mentioned here.

7. References

[1] Priestly MJN, Tao J (1993): Seismic response of precast prestressed concrete frames with partially debonded tendons. *PCI Journal*, **38**(1), 58-69.

[2] Stanton JF, Stone WC, Cheok GS (1997): A hybrid reinforced precast frame for seismic regions. *PCI Journal*, **42**(2), 20-32.

[3] Bradley BA, Dhakal RP, Mander JB, Li L (2008): Experimental multi-level seismic performance assessment of 3D RC frame designed for damage avoidance. *Earthquake Engineering & Structural Dynamics*, **37**(1), 1–20.

[4] Toranzo LA (2002): The use of rocking walls in confined masonry structures: a performance-based approach. *Ph.D. Thesis*, University of Canterbury, Christchurch, New Zealand.

[5] Palermo A, Pampmanin S, Buchanan A (2006): Experimental investigations on LVL seismic resistant wall and frame subassemblies. *First European Conference on Earthquake Engineering and Seismology*, Geneva, Switzerland.

[6] Eatherton MR, Ma X, Krawinkler H, Mar D, Billington S, Hajjar JF, Deierlein GG (2014): Design concepts for controlled rocking of self-centering steel-braced frames. *Journal of Structural Engineering*, **140**(11).

[7] Priestly MJN, Sritharan S, Conley J, Pampanin S (1999): Preliminary results and conclusions from the PRESSS five-story precast concrete test building. *PCI Journal*, **44**(6), 42–67.

[8] Perez FJ, Pessiki S, Sause R (2013): Experimental lateral load response of unbonded post-tensioned precast concrete walls. *ACI Structural Journal*, **110**(6), 1045-1053.

[9] Henry RS, Brooke NJ, Sritharan S, Ingham JM (2012): Defining concrete compressive strain in unbonded post-tensioned walls. *ACI Structural Journal*, **109**(1), 101-112.

[10] Holden T, Restrepo J, Mander JB (2003): Seismic performance of precast reinforced and prestressed concrete walls. *Journal of Structural Engineering*, **129**(3), 286-296.

[11] Restrepo JI, Rahman A (2007): Seismic performance of self-centering structural walls incorporating energy dissipators. *Journal of Structural Engineering*, **133**(11), 1560-1570.

[12] Smith B, Kurama Y, McGinnis M (2012). Hybrid precast wall systems for seismic regions. *Structural Engineering Research Report #NDSE-2012-01*, University of Notre Dame, IN.

[13] Marriott D, Pampanin S, Palermo A (2009): Quasi-static and pseudo-dynamic testing of unbonded post-tensioned rocking bridge piers with external replaceable dissipaters. *Earthquake Engineering & Structural Dynamics*, **38**(3), 331-354.

[14] ACI Innovation Task Group 5 (2009): Requirements for design of a special unbonded post-tensioned precast shear wall satisfying ACI ITG-5.1 (ITG 5.2-09). *ACI*, Farmington Hills, MI.

[15] ACI 550.3-13 (2014): Design specification for unbonded post-tensioned precast concrete special moment frames satisfying ACI 374.1. *ACI*, Farmington Hills, MI.

[16] Pampanin S, Priestley MJN, Sritharan S. (2001): Analytical modeling of the seismic behavior of precast concrete frames designed with ductile connections. *Journal of Earthquake Engineering*, 5(3), 329-367.

[17] Aaleti S, Sritharan S (2009): A simplified analysis method for characterizing unbonded post-tensioned precast wall systems. *Engineering Structures*, **31**, 2966-2975.

[18] Palermo A, Pampanin S, Carr AJ (2005): Efficiency of simplified alternative modelling approaches to predict the seismic response of precast concrete hybrid systems. *fib Symposium 2005: "Keep Concrete Attractive"*, Budapest, Hungary.

[19] Kurama Y, Sause R, Pessiki S, Lu LW (1999): Lateral load behavior and seismic design of unbonded post-tensioned precast concrete walls. *ACI Structural Journal*, **96**(4), 622-632.

[20] Perez FJ, Sause R, Pessiki S (2007): Analytical and experimental lateral load behavior of unbonded post-tensioned precast concrete walls. *Journal of Structural Engineering*, **133**(11), 1531-1540.

[21] Nagae T, Tahara K, Taizo M, Shiohara H, Kabeyasawa T, Kono S, Nishiyama M, Wallace JW, Ghannoum WM, Moehle JP, Sause R, Keller W, Tuna Z (2011): Design and instrumentation of the 2010 E-Defense four-story reinforced concrete and post-tensioned concrete buildings. *PEER Report 2011/104*, Berkeley, CA.

[22] Tuna Z, Gavridou S, Wallace JW, Nagae T, Matsumori T (2014): 2010 E-Defense four-story reinforced concrete and post-tensioned buildings - comparative study of experimental and analytical results. *Proc. 10th National Conf. in Earthquake Eng.*, Earthquake Eng. Research Institute, Anchorage, AK.

[23] Gavridou S. (2015): Shake table testing and analytical modeling of a full-scale, four-story unbonded post-tensioned concrete wall building. *Ph.D. Dissertation*, University of California, Los Angeles.

[24] Thomas DJ, Sritharan S (2004): An evaluation of seismic design guidelines proposed for precast jointed wall systems. *ISU-ERI-Ames Report ERI-04643*, Iowa State University, Ames, Iowa.

[25] Panagiotou M, Restrepo JI, Conte JP (2011): Shake-table test of a full-scale 7-story building slice. Phase I: Rectangular wall. *Journal of Structural Engineering*, **137**(6), 691–704.

[26] CSI Perform-3D V5 (2011): Nonlinear analysis and performance assessment for 3D structures, *Computer and Structures, Inc*, Berkeley, CA.